6 Watt Segmented Power Generator Modules using Bi_2Te_3 and $(InGaAs)_{1-x}(InAlAs)_x$ Elements Embedded with ErAs Nanoparticles.

Gehong Zeng[1], Je-Hyeong Bahk[1], Ashok T. Ramu[1], John E. Bowers[1], Hong Lu[2], Arthur C. Gossard[2] Zhixi Bian[3], Mona Zebarjadi[3] and Ali Shakouri[3]

[1]Department of Electrical and Computer Engineering, University of California, Santa Barbara, CA 93106, U.S.A.
[2]Materials Department, University of California, Santa Barbara, CA 93106, U.S.A.
[3]Electrical Engineering Department, University of California, Santa Cruz, CA 95064, U.S.A.

ABSTRACT

We report the fabrication and characterization of segmented element power generator modules of 16 x 16 thermoelectric elements consisting of 0.8 mm thick Bi_2Te_3 and 50 μm thick $ErAs:(InGaAs)_{1-x}(InAlAs)_x$ with 0.6% ErAs by volume. Erbium Arsenide metallic nanoparticles are incorporated to create scattering centers for middle and long wavelength phonons, and to form local potential barriers for electron filtering. The thermoelectric properties of $ErAs:(InGaAs)_{1-x}(InAlAs)_x$ were characterized in terms of electrical conductivity and Seebeck coefficient from 300 K up to 830 K. Generator modules of Bi_2Te_3 and $ErAs:(InGaAs)_{1-x}(InAlAs)_x$ segmented elements were fabricated and an output power of 6.3 W was measured. 3D finite modeling shows that the performance of thermoelectric generator modules can further be enhanced by the improvement of the thermoelectric properties of the element materials, and reducing the electrical and thermal parasitic losses.

INTRODUCTION

Solid state thermoelectric generator modules composed of n and p semiconductor element couples can be used for directly thermal to electrical energy conversion. Their great potential in providing cleaner form of energy and reducing environmental contamination has been recognized. The power conversion performance of a thermoelectric generator module depends on the semiconductor's thermoelectric properties, in terms of the figure of merit, $Z = \alpha^2 \cdot \sigma / \kappa$, where α is the Seebeck coefficient, σ is the electrical conductivity and κ is the thermal conductivity. Thermal conductivity can be reduced due to the increase of phonon scattering by abundant surfaces and interfaces in nanostructured materials, and the Seebeck coefficient can be increased through thermionic emission across heterointerfaces,[1] and/or electron scattering by nanostructures.[2, 3] Thermal conductivity reduction using superlattice heterostructures or incorporation of nanoparticles has been demonstrated [4, 5]. When ErAs nanoparticles are incorporated into $(InGaAs)_{1-x}(InAlAs)_x$, potential barriers are formed at the interface between the particle and semiconductor. The Seebeck coefficient can therefore be enhanced through the electron filtering effects of these potential barriers.[6] The performance of a solid state generator also depends on the Carnot efficiency, which can be expressed as $\Delta T/T_h$., where ΔT is the temperature difference across the elements, and T_h the hot side temperature of the elements. Large ΔT is desirable for large output power and high

efficiency. The performance of a thermoelectric generator module can be effectively enhanced by using segmented element structures with materials whose thermoelectric properties are optimized in successive temperature ranges,

In this paper, we report the fabrication, characterization and measurement of generator modules using segmented elements of 50 μm $(InGaAs)_{1-x}(InAlAs)_x$ and 0.8 mm Bi_2T_3. The generator modules were fabricated via the pick-up and place method, and flip-chip bonding technique. An output power of 6.3 W was measured with a heat source temperature at 610 K.

MATERIAL CHARACTERIZATION

Two 50 μm 0.6% $ErAs:(InGaAs)_{1-x}(InAlAs)_x$ samples for segmented generator modules were grown lattice-matched on InP(100) substrates of 520 μm thick using MBE. The growth rate was about 2 μm per hour and the growth temperature was maintained at 490 °C. The n-type $ErAs:(InGaAs)_{1-x}(InAlAs)_x$ consists of 80% InGaAs and 20%InAlAs, while the p-type sample is ErAs:InGaAs.

Characterization samples of $(InGaAs)_{0.8}(InAlAs)_{0.2}$ of 2 μm thick with 0.6% Er with the same material structure as that of the 50 μm material were grown on semi-insulating InP substrates of about 520 μm thick via MBE for the Seebeck coefficient and electrical conductivity measurements. To avoid side effects from InP substrate in electrical conductivity and Seebeck coefficient measurements at high temperatures, the semi-insulating InP substrate was removed in our material characterization. The epitaxial sample was bonded onto sapphire substrate using a SiO_2-SiO_2 oxide bonding technique. Then, the semi-insulating InP was removed by wet etching leaving just the 2 μm epitaxial layer of 0.6%Er $(InGaAs)_{0.8}(InAlAs)_{0.2}$ bonded on a 500 μm sapphire substrate. A Van der Pauw device pattern was formed on the 2 μm epitaxial layer by reactive ion etching. Metallization of TiWN was used as metal diffusion barrier, which showed very good Au barrier property and thermal stability up to 700 C. [7] The measurements were carried out in a vacuum chamber with the pressure pumped below 1 mTorr. The measurement results in figure 1 show that the Seebeck coefficient increases with temperature.

The electrical conductivity was measured using the same Van der Pauw device pattern as the
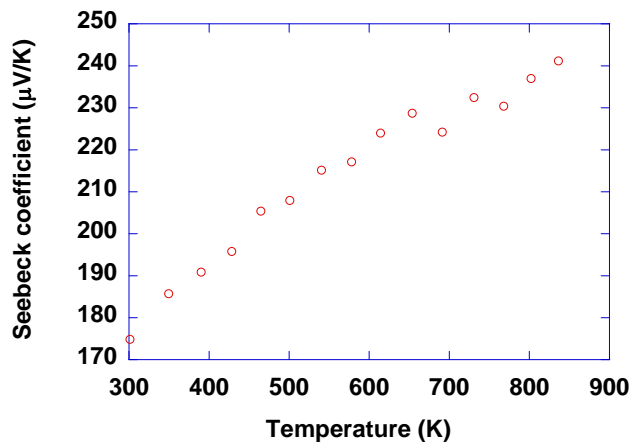
Figure 1. Measurement results of Seebeck coefficients of $(InGaAs)_{0.8}(InAlAs)_{0.2}$ with 0.6% ErAs nanoparticles from 300 K to 830 K.
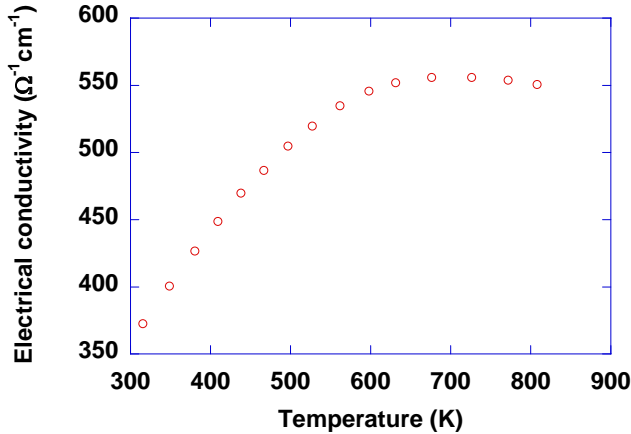
Figure 2. Measurement results of electrical conductivity of $(InGaAs)_{0.8}(InAlAs)_{0.2}$ with 0.6% ErAs nanoparticles from 300 K up to 800 K.

one used for Seebeck coefficient measurements. In electrical conductivity measurements, the device was placed in the center of one copper heater bar in the vacuum chamber. Two current and two voltage electrodes were connected to the four metal pads of the device, and data acquisition were done via a control computer. The Van der Pauw pattern is a cloverleaf shape, and four electrodes were placed at the far corners of the pattern, so the measurement errors from pattern geometry were almost negligible. Fig. 2 shows the measurement results with temperatures from 300 K up to 800 K.

DEVICE FABRICATION

The segmented generator modules were fabricated via pick-up and place approach method and flip-chip bonding techniques. Processing techniques are similar to those of standard large scale integrated circuits for the segmented elements of ErAs:InGaAlAs and Bi_2Te_3. The thin film element fabrication started with the front side metallization of the epitaxial layer: Ni/GeAu/Ni/Au contact metals were used for n-type ErAs:InGaAlAs, and Pt/Ti/Pt/Au were used for p-type ErAs:InGaAs, respectively. The InP substrate was removed through wet etching solution to expose the backside of the 50 μm epitaxial layer. The backside metallization was also the same Ni/GeAu/Ni/Au and Pt/Ti/Pt/Au were used for n-type and p-type, respectively. Then the n and p type thin film wafers were diced into 1.4 mm × 1.4 mm square chips ready for bonding. Ni was used as contact metallization for Bi_2Te_3 of both n and p type. The bulk Bi_2Te_3 was cut into square chips of 1.4 mm × 1.4 mm in area. All the Bi_2Te_3 elements were bonded on a lower ceramic plate; while the ErAs:InGaAlAs elements were bonded on an upper ceramic plate. Finally, the lower Bi_2Te_3 bonded plate and the upper ErAs:InGaAlAs bonded plate were bonded together using flip-chip bonding to form a 16 x 16 element generator module.

## MEASUREMENT RESULTS AND DISCUSSIONS

The measurement setup consists of a heat sink with circulating cooling water, a heat source of aluminum block with two built-in electrical cartridge heaters, two thermocouples for temperature monitoring, and electrical probes for the output power measurements. One of the thermocouples was fixed in the aluminum heat source block, 1 mm away from the interface of the heat block and
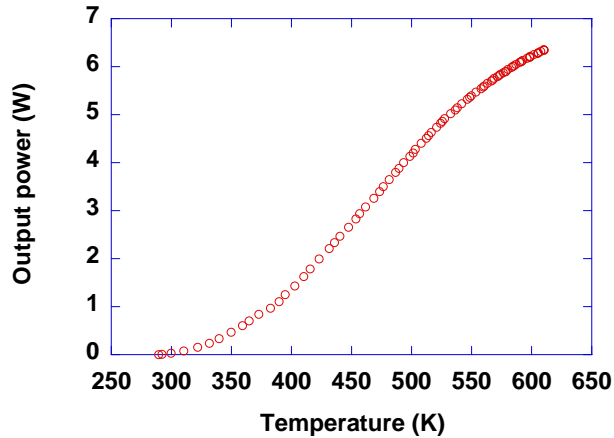
Figure 3. The output power measurement results for the 16 x 16 segment element power generator of 50 µm ErAs:(InGaAs)$_{1-x}$(InAlAs)$_x$ and 0.8 mm Bi$_2$Te$_3$. The data were obtained when the heat source temperature was increased from 290 K up to 610 K.

generator ceramic plate and used as the heat source temperature sensor; the other was placed on the heat sink surface at the interface of the heat sink and the generator as heat sink temperature sensor. The cooling water temperature was set at 285 K. The measurement results of output power are shown in Figure 3. In the low temperature range when heat source temperature is below 450 K, the output power shows quadratic increase with temperature, but when the heat source temperature rises above 500 K, the output power begins to saturate, which indicates that the thermoelectric properties of Bi$_2$Te$_3$ degrade when the temperature is above 500 K. To get a better understanding of the performance of the segmented generator modules, a 3D finite element model (FEM) was set up for theoretical analyses. The thermoelectric effects of the Peltier, Seebeck and Thomson are all taken into account in our finite analyses, and the material property values, metal to semiconductor electrical contact resistances were from experimental results. The water circulating heat sink was modeled using a constant heat transfer coefficient at the cold side of the module. The external electrical load was a constant resistor which was made to be an impedance match to the module. An output voltage to the external electrical load resistor due to the thermoelectric properties of the segmented elements was obtained at each heat source temperature, therefore the output current and power to the load resistor at each heat source temperature becomes known. Figure 4 shows the 3D modeling result of the electric potential distribution across the generator module's element couple. As the n and p elements are electrically connected in series, and thermally connected in parallel, the highest potential is at the cold side of p-type element, (red area); lowest electric potential is at the cold side of n-type element (blue area).

A comparison of the 3D FEM values with measurement results is shown in Fig. 5. When temperature is below 500 K, the two results fit well. This indicates that in the low temperature range from 300 K to 500 K, the 3D model is close to the real generator module and its working conditions. When the temperature is above 500 K, measurements and finite element module results begin to show their discrepancy, which comes from the thermal resistance increasing at
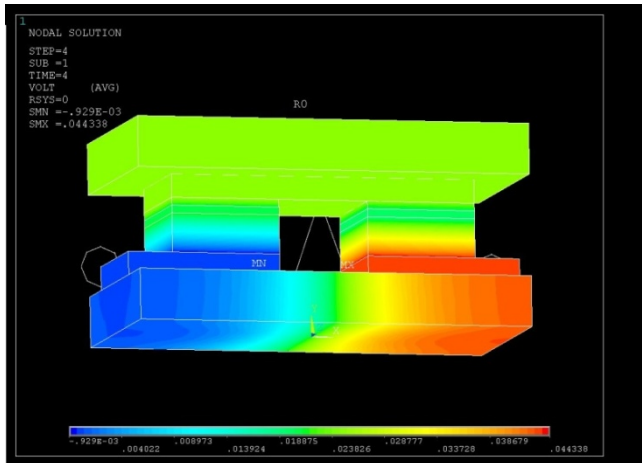
Figure 4. 3D simulation result shows the potential distribution across the module n and p elements when loaded with external electrical resistor R_o. The lowest potential is at cold side of the n-type segmented element leg; while the highest potential occurs at the cold side of the p-type segmented element.

the interface of heat source block and module as temperature rises, so the real temperature drop across the elements does not increase linearly with the rise of the heat source temperature. In the 3D model, the heat block on the top of the generator module was modeled as an ideal heat source at a constant temperature without any thermal interfaces at the interface between the heat source and the module. In real measurement setup, the interface of heat source and generator module was connected using thermal paste, which can quickly become dry at high temperatures and present larger thermal resistance, and therefore produce significant temperature drop at the interface. One solution to it is to use liquid metals instead of thermal paste for the hot side interface connection, such as indium or stannum, the thermal conductivity of which can be very high when melted at high temperatures. The optimization results of our finite element model also show that the output power can be improved by improving the thermoelectric properties of the
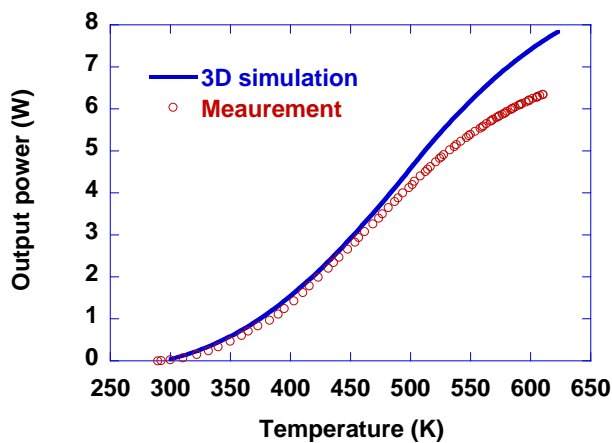
Figure 5. A comparison of 3D simulation values with real generator module measurements.

elements, reducing the thermal and electrical parasitic loss, and increasing heat transfer coefficient of the heat sink.

CONCLUSIONS

The incorporation of ErAs nanoparticles into $(InGaAs)_{1-x}(InAlAs)_x$ alloy results in significant improvement in the material's thermoelectric properties. Variable temperature measurements of 0.6% $ErAs:(InGaAs)_{1-x}(InAlAs)_x$ show that the Seebeck coefficient increases with temperature from 173 µV/K at 300 K up to 240 µV/K at 830 K, and electrical conductivity increases with temperature from 370 $\Omega^{-1}\cdot cm^{-1}$ at 300 K up to 550 $\Omega^{-1}\cdot cm^{-1}$ at 700 K. A 16×16 generator module was fabricated using segmented elements of 50 µm $0.6\% ErAs:(InGaAs)_{1-x}(InAlAs)_x$ and 0.8 mm Bi_2Te_3. An output power of 6.3 W was measured with heat source temperature at around 620 K. The 3D finite element modeling shows that the performance of thermoelectric generator modules can be further improved by improving material thermoelectric properties, reducing electrical and thermal parasitic resistance loss, and improving the heat transfer coefficient of the heat sink.

ACKNOWLEDGMENTS

REFERENCES

[1]   A. Shakouri and J. E. Bowers, "Heterostructure integrated thermionic coolers," *Applied Physics Letters,* vol. 71, pp. 1234-1236, SEP 1 1997.

[2]   S. V. Faleev and F. Leonard, "Theory of enhancement of thermoelectric properties of materials with nanoinclusions," *Physical Review B,* vol. 77, pp. -, Jun 2008.

[3]   M. Zebarjadi, K. Esfarjani, A. Shakouri, J.-H. Bahk, Z. Bian, G. Zeng, J. E. Bowers, H. Lu, J. M. O. Zide, and A. Gossard, *submitted to Applied Physics Letters* 2008.

[4]   R. Venkatasubramanian, E. Siivola, T. Colpitts, and B. O'Quinn, "Thin-film thermoelectric devices with high room-temperature figures of merit," *Nature,* vol. 413, pp. 597-602, OCT 11 2001.

[5]   W. Kim, S. L. Singer, A. Majumdar, D. Vashaee, Z. Bian, A. Shakouri, G. Zeng, J. E. Bowers, J. M. O. Zide, and A. C. Gossard, "Cross-plane lattice and electronic thermal conductivities of ErAs:InGaAs/InGaAlAs superlattices," *Applied Physics Letters,* vol. 88, p. 242107, 2006.

[6]   J. M. O. Zide, D. Vashaee, Z. X. Bian, G. Zeng, J. E. Bowers, A. Shakouri, and A. C. Gossard, "Demonstration of electron filtering to increase the Seebeck coefficient in In0.53Ga0.47As/ In0.53Ga0.28Al0.19As superlattices," *PHYSICAL REVIEW B,* vol. 74, p. 205335, 2006.

[7]   S. Bhagat, H. Han, and T. L. Alford, "Tungsten-titanium diffusion barriers for silver metallization," *Thin Solid Films,* vol. 515, pp. 1998-2002, Dec 5 2006.